

## CORONAVIRUS

# Severe COVID-19 induces autoantibodies against angiotensin II that correlate with blood pressure dysregulation and disease severity

Priscilla S. Briquez<sup>1,2</sup>, Sherin J. Rouhani<sup>3</sup>, Jovian Yu<sup>3</sup>, Athalia R. Pyzer<sup>3</sup>, Jonathan Trujillo<sup>3</sup>, Haley L. Dugan<sup>4,5</sup>, Christopher T. Stamper<sup>4,5,6</sup>, Siriruk Changrob<sup>4</sup>, Anne I. Sperling<sup>5,7,8</sup>, Patrick C. Wilson<sup>4,5</sup>, Thomas F. Gajewski<sup>3,5,9,10</sup>, Jeffrey A. Hubbell<sup>1,5,10</sup>, Melody A. Swartz<sup>1,5,9,10\*</sup>

Patients infected with the severe acute respiratory syndrome coronavirus 2 (SARS-CoV-2) can experience life-threatening respiratory distress, blood pressure dysregulation, and thrombosis. This is thought to be associated with an impaired activity of angiotensin-converting enzyme 2 (ACE2), which is the main entry receptor of SARS-CoV-2 and which also tightly regulates blood pressure by converting the vasoconstrictive peptide angiotensin II (AngII) to a vasopressor peptide. Here, we show that a significant proportion of hospitalized patients with COVID-19 developed autoantibodies against AngII, whose presence correlates with lower blood oxygenation, blood pressure dysregulation, and overall higher disease severity. Anti-AngII antibodies can develop upon specific immune reaction to the SARS-CoV-2 proteins Spike or receptor-binding domain (RBD), to which they can cross-bind, suggesting some epitope mimicry between AngII and Spike/RBD. These results provide important insights on how an immune reaction against SARS-CoV-2 can impair blood pressure regulation.

## INTRODUCTION

Severe acute respiratory syndrome coronavirus 2 (SARS-CoV-2), the causative virus of coronavirus disease 2019 (COVID-19), infects cells by binding to angiotensin-converting enzyme 2 (ACE2) via the receptor-binding domain (RBD) of its Spike protein. ACE2 is an enzyme expressed on the surfaces of alveolar epithelial cells and vascular endothelial cells (1), among others, that plays an important role in regulating blood pressure (BP) by converting the vasoconstrictive peptide angiotensin II (AngII) to the vasopressor peptide angiotensin-(1-7) (2, 3). It is known that SARS-CoV-2 infection can lead to dysregulation of vascular tension, endothelial inflammation, and enhanced thrombosis, presumably through enhancing endocytosis of ACE2 and thereby lowering its cell surface presence (4, 5).

Here, we sought to explore whether SARS-CoV-2 infection might induce autoantibodies against the peptide AngII. We hypothesized that the simultaneous binding of SARS-CoV-2 and AngII to ACE2 might lead to their coprecipitation by antigen-presenting cells, thus providing a strong immune adjuvant (the virus molecules) to the self-peptide AngII, leading to an anti-AngII autoimmune response (6, 7). Moreover, we asked whether some epitope mimicry might exist between a domain on the Spike protein and AngII, based on their shared binding to ACE2. The induction of anti-AngII antibodies in patients with COVID-19, if it occurs, could interfere with AngII

processing by ACE2 and signaling to its receptors, potentially contributing to the dysregulation of vascular tension and worsening acute respiratory distress syndrome (8, 9).

We conducted observational studies using serum of hospitalized patients with COVID-19 and determined that such autoantibodies are indeed induced, independently of anti-RBD levels. Instead, their presence and levels were strongly correlated with BP dysregulation and poor oxygenation. We lastly demonstrated cross-reactivity of some antibodies between AngII and the Spike protein, suggesting immune epitope homology between these molecules.

## RESULTS AND DISCUSSION

We began by assessing the presence of immunoglobulin G (IgG) antibodies against AngII in the plasma of 221 subjects, among which 115 were hospitalized patients with COVID-19, 58 were control donors (from nonhypertensive patients sampled before the pandemic), and 48 were hypertensive non-SARS-CoV-2-infected donors (sampled before the pandemic). Of the patients with COVID-19, 75 had plasma taken at multiple times after symptom onset. Unexpectedly, we found that a majority (63%, 73 of 115) of the patients with COVID-19 had positive levels of anti-AngII autoantibodies, as determined by an enzyme-linked immunosorbent assay (ELISA) absorbance greater than 3 SDs above the mean of the control donor group (Fig. 1A). Of these, 53% (39 of 73) had high levels, defined as greater than twice the positive threshold. In contrast, only one control donor (1.7%) was anti-AngII positive, with a level just above the positive limit. Of the 59 anti-AngII(+) patients with multiple time points, 37% developed positive levels of anti-AngII after earlier testing negative, 30% lost the antibodies after testing positive, and the rest (32%) were positive at all tested time points (Fig. 1B). This demonstrates that antibodies against AngII can both develop and disappear over time during the course of infection and disease.

Because a majority of the hospitalized patients with COVID-19 in this cohort had preexisting hypertension (HTN) (COVID HTN, 64%),

<sup>1</sup>Pritzker School for Molecular Engineering, University of Chicago, Chicago, IL, USA.

<sup>2</sup>Department of General and Visceral Surgery, Medical Center—University of Freiburg,

Faculty of Medicine, University of Freiburg, Freiburg 79106, Germany. <sup>3</sup>Department

of Medicine, Section of Hematology/Oncology, University of Chicago, Chicago, IL,

USA. <sup>4</sup>Department of Medicine, Section of Rheumatology, University of Chicago,

Chicago, IL, USA. <sup>5</sup>Committee on Immunology, University of Chicago, Chicago, IL, USA.

<sup>6</sup>Center for Infectious Medicine, Department of Medicine Huddinge, Karolinska

Institutet, Karolinska University Hospital Huddinge, Stockholm, Sweden. <sup>7</sup>Department

of Medicine, Section of Pulmonary and Critical Care Medicine, University of

Chicago, Chicago, IL, USA. <sup>8</sup>Department of Medicine, Department of Pulmonary

and Critical Care Medicine, University of Virginia, Charlottesville, VA, USA. <sup>9</sup>Ben May

Department of Cancer Research, University of Chicago, Chicago, IL, USA. <sup>10</sup>Com-

mittee on Cancer Biology, University of Chicago, Chicago, IL, USA.

\*Corresponding author. Email: melodyswartz@uchicago.edu

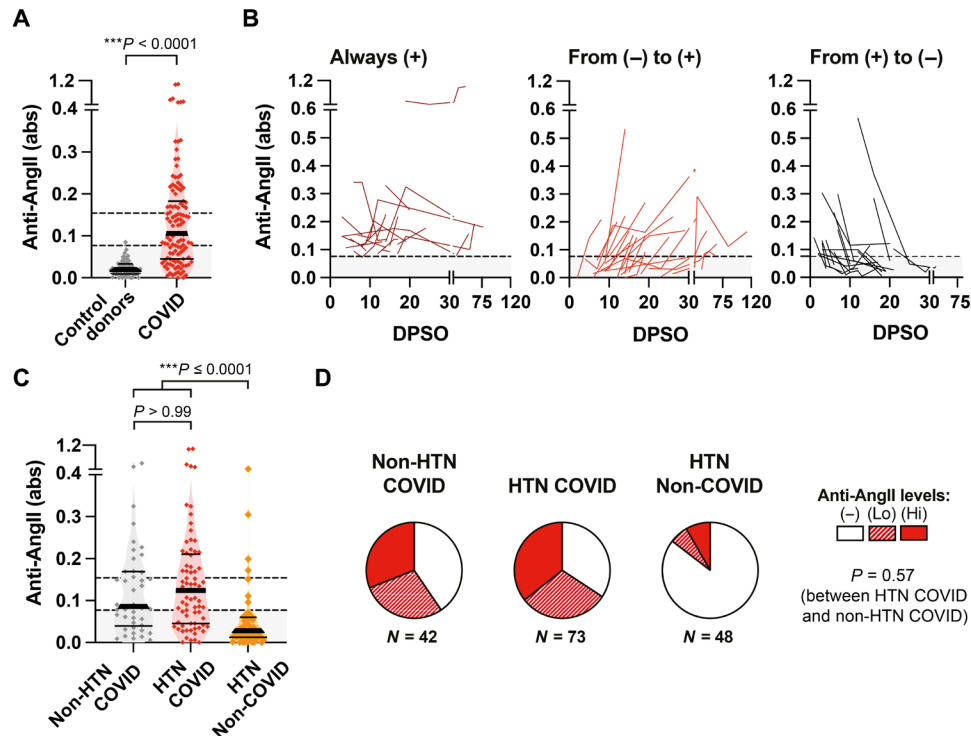


**Fig. 1. SARS-CoV-2 infection induces anti-AngII autoantibodies in a majority of hospitalized patients.** The plasma of SARS-CoV-2 convalescent hospitalized patients (COVID,  $N = 115$ ) was analyzed for the presence of anti-AngII by ELISA. For 75 of them, multiple time points were available and analyzed. Among the patients with COVID, 63% had preexisting HTN (HTN COVID,  $N = 73$ ). Results were compared to non-COVID hypertensive donors (non-COVID HTN,  $N = 48$ ) or control donors ( $N = 58$ ). Anti-AngII levels are displayed as the signal absorbance (abs) measured in plasma diluted at 1:100. (A) Levels of anti-AngII antibodies in the plasma of patients with COVID as compared to control donors (median  $\pm$  IQR, Mann-Whitney test). Absorbance of  $\geq 0.077$  and  $\geq 0.154$  indicates the limit for anti-AngII positivity and high levels, respectively. (B) Analysis of anti-AngII in patients with COVID at multiple time points. Patients were separated in three groups: patients who were anti-AngII positive at all analyzed time points [always (+), left], patients who were anti-AngII (-) and turned anti-AngII(+) during the course of the disease [from (-) to (+), middle], and patients who were anti-AngII(+) and who became anti-AngII(-) [from (+) to (-), right]. Each line represents an individual patient. (C) Levels of anti-AngII in COVID patients with or without preexisting HTN compared to non-COVID HTN patients (median  $\pm$  IQR, Kruskal-Wallis test with Dunn's posttest). (D) Proportion of non-HTN COVID, HTN COVID, and non-COVID HTN patients who have high (Hi), low (Lo), or negative (-) levels of anti-AngII ( $\chi^2$  test comparing non-HTN and HTN COVID patients).

we measured anti-AngII levels in plasma from hypertensive donors taken before the pandemic (non-COVID HTN) to determine whether autoantibodies against AngII could have been preexisting in patients with HTN. We detected anti-AngII antibodies in 15% of these hypertensive donors (Fig. 1C). However, when comparing the HTN versus non-HTN COVID-19 patients, the levels of anti-AngII were similar (Fig. 1C) as well as the percentages with positive levels (65 and 60%, respectively; Fig. 1D). These results, together with the data shown in Fig. 1B, indicate that infection with SARS-CoV-2 promotes the development of anti-AngII IgG antibodies in most of the patients with COVID who required hospitalization, regardless of whether they had preexisting HTN.

In addition to preexisting HTN, we found no significant correlations between anti-AngII positivity and patient age, sex, or body mass index (BMI) (fig. S1, A to D), although older patients trended toward increased levels of anti-AngII ( $P = 0.064$  by Spearman correlation; fig. S1A). Additional trends suggested that female patients with COVID-19 were more likely to develop high anti-AngII levels (42% versus 25% of males; fig. S1B) as well as patients with BMI  $\geq 25$  (38% versus 20% of patients with normal BMI; fig. S1, C and D).

Next, we asked whether the presence and levels of anti-AngII antibodies correlated with those of antibodies directed against the RBD

of the virus' Spike protein. As expected, most patients (76%) developed positive levels of anti-RBD antibodies, here considered above a total IgG titer of 3 based on healthy control levels (fig. S2A). However, correlations between anti-RBD levels and anti-AngII levels were only modest; a majority of anti-AngII(-) patients developed antibodies against RBD (Fig. 2A), and patients with high anti-RBD titers did not necessarily develop anti-AngII antibodies [34% remained anti-AngII(-)] (Fig. 2B). In addition, although patients positive for one antibody were more likely to be positive for the other, this effect was not statistically significant [ $P = 0.056$  and  $P = 0.087$  using  $\chi^2$  tests comparing the proportion of anti-AngII(+) patients across the anti-RBD (-/Lo/Hi) groups and vice versa]. A weak correlation was nevertheless observed when considering the average antibody levels instead of proportions of positive patients ( $R = 0.21$ ,  $P = 0.009$  by Spearman correlation) (Fig. 2C and fig. S2, B and C).

We then questioned when anti-AngII antibodies developed relative to anti-RBD antibodies after SARS-CoV-2 infection by comparing their levels between earlier [1 to 10 days post-symptom onset (DPSO)] versus later (11 to 20 DPSO) times in the 25 anti-AngII(+) patients for which these time points were available. Notably, the fact that some patients were already anti-AngII(+) at an early time after symptom (Fig. 1B) did not necessarily imply that these antibodies

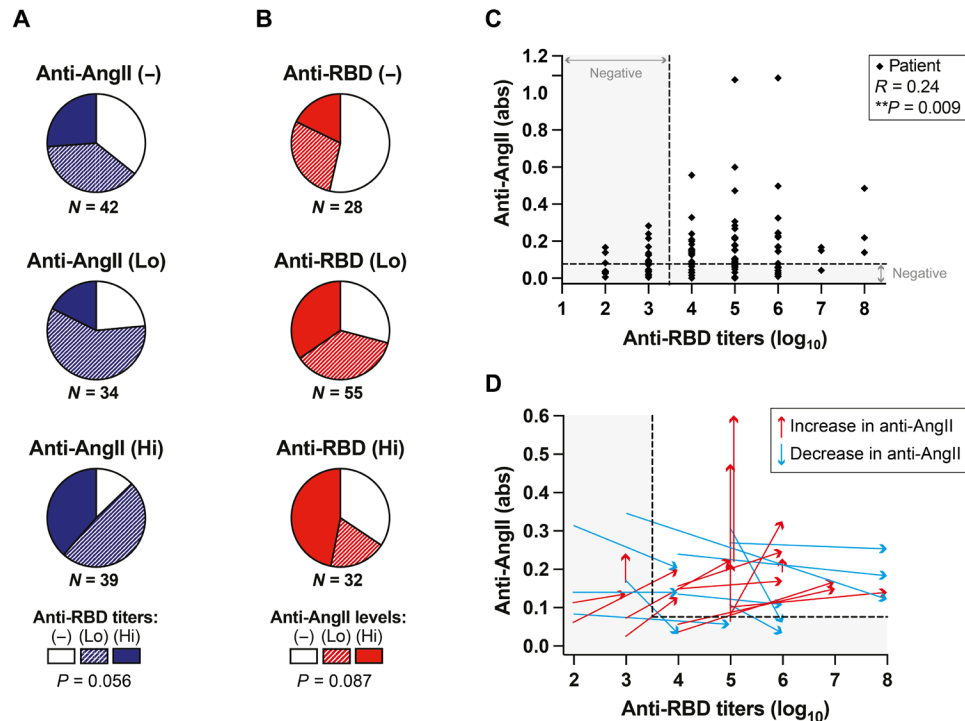


**Fig. 2. Relationship between anti-AngII and anti-RBD antibodies in COVID-hospitalized patients.** Anti-RBD antibodies were titrated in the plasma of SARS-CoV-2 convalescent hospitalized patients (COVID,  $N = 115$ ), in addition to anti-AngII autoantibodies. Anti-RBD titers are displayed as  $\log_{10}$  values [Hi = high (titers 6 to 8); Lo = low (titers 4 to 5); and (-) = negative (titer <4); gray thresholds = limits for anti-AngII or anti-RBD positivity]. Gray threshold indicates positivity of anti-AngII and anti-RBD. (A) Proportion of patients with high, low, or no titers of anti-RBD among patients having high, low, or negative levels of anti-AngII ( $\chi^2$  test). (B) Proportion of patients with high, low, or negative levels of anti-AngII among patients having high, low, or no titers of anti-RBD ( $\chi^2$  test). (C) Correlation between anti-AngII levels and anti-RBD titers in patients with COVID (Spearman correlation). (D) Covariations of anti-AngII and anti-RBD levels between 1 to 10 DPSO (tail of the arrow) and 11 to 20 DPSO (tip of the arrow) matched per patient (arrow,  $N = 25$ ).

were preexisting before SARS-CoV-2 infection, as highlighted by the presence of anti-RBD at early times as well (fig. S2, D and E). The incubation period of SARS-CoV-2 before symptom onset has been shown to be around 5.2 days (95% confidence interval: 4.1 to 7 days) during which immune responses against the virus are triggered (10, 11). From early to late, some patients showed increases in both anti-RBD and anti-AngII (15 of 25; Fig. 2D in red and fig. S2F), while others showed increases in anti-RBD accompanied by decreases in anti-AngII (10 of 25; Fig. 2D in blue and fig. S2G). Between these times, the increase in anti-RBD levels reached statistical significance (fig. S2D), as expected, whereas the increase in anti-AngII levels did not ( $P = 0.18$  by Wilcoxon matched pairs signed-rank test; fig. S2E). Together with the data shown in Figs. 1B and 2C, these data suggest that antibodies generated against AngII are lower affinity and more transient than those against RBD; this is not unexpected given that AngII is a short peptide (eight amino acids). Nevertheless, anti-AngII antibodies were still detected in 11 patients at >45 DPSO (fig. S2H), suggesting that anti-AngII antibodies could persist over long periods, or recur, in a subset of patients.

We next studied the development of anti-AngII IgG in mice upon exposure to SARS-CoV-2 antigens, noting that murine and human AngII are 100% homologous. We vaccinated mice at 0 and 21 days with 10  $\mu$ g of Spike or RBD, admixed with either (i) the Toll-like receptor 4 (TLR4) agonist monophosphoryl lipid A in alum [MPLA/alum, mimicking the AS04 (adjuvant system 4) clinical adjuvant], (ii) AddaS03 (a formulation composed of  $\alpha$ -tocopherol, squalene, and

polysorbate 80 in an oil-in-water nanoemulsion, mimicking the AS03 clinical adjuvant), (iii) the TLR9 agonist CpG-B, or (iv) no adjuvant. None of the naïve mice (0 of 25) had detectable anti-AngII IgG (Fig. 3A). In contrast, 24% (6 of 25) of the mice vaccinated with RBD + MPLA/alum and 27% (4 of 15) of the mice vaccinated with Spike + MPLA/alum developed antibodies against AngII. None of the mice vaccinated with Spike + AddaS03 (0 of 9) or with RBD + CpG (0 of 10) developed anti-AngII antibodies, as well as none of the mice vaccinated with unadjuvanted RBD or Spike (0 of 10 each), or with MPLA/alum lacking antigen (0 of 20).

We further analyzed the time course of the immune responses in mice, measuring anti-AngII levels at weeks 1, 2, 3, and 4 for the mice vaccinated with RBD + MPLA/alum or Spike + MPLA/alum that were positive for anti-AngII. This analysis highlighted an increase in anti-AngII levels over time, specifically between weeks 1 and 2 and week 4 after vaccination (Fig. 3B). Notably, the increase in anti-AngII IgG titers was more substantial after the vaccination boost at week 3. These results demonstrate that anti-AngII autoantibodies can be induced in mice by vaccination against Spike or RBD, in the absence of SARS-CoV-2 infection, at least with MPLA/alum-containing adjuvants.

Having determined that anti-AngII antibodies could develop both in hospitalized patients with COVID-19 and in mice after vaccination with MPLA/alum-adjuvanted SARS-CoV-2 antigens, we further examined hospitalized patients with COVID-19 for potential correlative effects of anti-AngII antibodies on BP dysregulation and disease severity as indicated by blood oxygenation. First, we observed

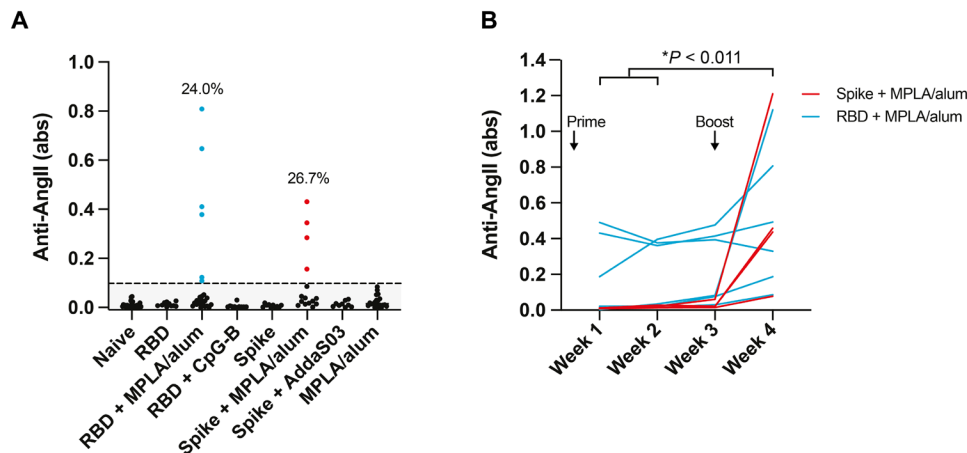


**Fig. 3. Development of anti-AngII autoantibodies in a subset of mice vaccinated with adjuvanted SARS-CoV-2 antigens.** Mice were vaccinated at weeks 0 and 3 with Spike or RBD proteins adjuvanted with MPLA/alum, CpG-B, AddaS03, or with no adjuvant, or with MPLA/alum only (in the absence of SARS-CoV-2 antigen).  $N = 10$  to 25 mice per group. **(A)** Anti-AngII levels in vaccinated mice plasma at week 4. Significant proportions of mice vaccinated with RBD + MPLA/alum or Spike + MPLA/alum raised autoantibodies against AngII (Z test for proportions: RBD + MPLA/alum versus MPLA/alum:  $Z = 2.35$ , Spike + MPLA/alum versus MPLA/alum:  $Z = 2.45$ ,  $*P < 0.038$  for both comparisons, gray threshold = limit for anti-AngII positivity). **(B)** Levels of anti-AngII autoantibodies over time (at weeks 1 to 4) in the mice that were found positive for anti-AngII at week 4 (Friedman test with Dunn's posttest).

that the levels of anti-AngII were significantly higher in patients with dysregulated BP, as defined by (i) episodes of hypotension that required administration of vasopressors, (ii) large daily fluctuations in BP [daily mean arterial pressure range ( $\Delta$ MAP)  $\geq 70$  mmHg], or (iii) at least two consecutive days of hypotension (MAP  $< 65$  mmHg) in patients with preexisting HTN (Fig. 4A). Moreover, this correlation remained significant when each of these subgroups was analyzed separately (Fig. 4B) (noting that these three subgroups are not exclusive, with 52% of patients belonging to multiple categories). Consistent with these observations, a majority of patients with BP dysregulation were positive for anti-AngII (81% versus 53% in patients with normal BP; Fig. 4C), among which 45% had high levels of anti-AngII. Last, patients needing vasopressors were the most likely to have positive or high levels of anti-AngII, although among each of the groups with dysregulated BP,  $>80\%$  were anti-AngII(+) (Fig. 4D).

Furthermore, we wondered whether the level of anti-AngII antibodies in COVID-19 patients with dysregulated BP was affected by their preexisting HTN status. Nevertheless, we found no notable difference between the non-HTN and HTN subsets that could support that patients with dysregulated BP were most likely to have positive or high anti-AngII levels when suffering from preexisting HTN (Fig. 4E).

Next, we asked whether the presence or levels of anti-AngII antibodies correlated with reduced blood oxygenation and disease severity, measured via the daily mean oximetric saturation (SF ratio), which is the ratio of peripheral oxygen saturation ( $\text{SpO}_2$ ) to the fraction of inspired oxygen ( $\text{FiO}_2$ ). For each patient, we selected the lowest daily mean SF ratio value obtained within a 2-day window of the measurement of anti-AngII (or the highest anti-AngII level for patients with multiple time points). The lowest daily mean SF ratio was compared between the patients with COVID-19 who developed autoantibodies against AngII versus those who did not. We found that the SF ratio was strongly reduced in anti-AngII(+) patients (Fig. 5A), demonstrating a correlation between anti-AngII antibodies and reduced blood oxygenation in these patients.

Because the clinical severity of COVID directly depends on the patient's blood oxygenation, patients with SF ratio  $\geq 314$  are considered

as having a disease of low severity, while patients with SF ratio  $< 235$  suffer from a highly severe form of COVID. On the basis of this, we then compared average anti-AngII levels among the three disease severity groups and found that patients with severe versus mild disease trended toward higher levels of anti-AngII antibodies ( $P = 0.053$ ; Fig. 5B). More notably, when looking at fractions of patients with anti-AngII positivity among each group, we found a significant increase in the proportions of anti-AngII(+) patients along with disease severity ( $P = 0.035$  by  $\chi^2$  test; Fig. 5C). Seventy-seven percent of patients with severe disease were anti-AngII(+), including 41% with high levels, as compared to 50 and 29%, respectively, in patients with mild disease.

To further rule out the possibility that AngII could have been preexisting in patients with more severe disease, we considered the three subgroups of anti-AngII(+) patients with multiple time points (shown in Fig. 1B), comparing SF ratios at the later time points. Between those patients who were positive for anti-AngII antibodies at all times tested (Fig. 5D, left) and those who developed positive levels after first testing negative (Fig. 5D, middle), similar fractions had mild, moderate, and severe levels of SF ratios at the later time points. However, in patients whose anti-AngII antibody levels went from positive to negative (Fig. 5D, right), most had improved SF ratios, with a majority (72%) showing high blood oxygenation (mild disease) and none with severe levels ( $P = 0.034$  by  $\chi^2$  test).

Together, these results demonstrate significant correlations between the presence and levels of anti-AngII in patients with COVID-19 and dysregulated BP, lower blood oxygenation, and increased disease severity. While causal relationships cannot be drawn from these correlations, the fact that AngII is a key regulator of BP in humans suggests that antibodies directed against anti-AngII could alter AngII signaling pathways, including its binding to and signaling via the angiotensin receptors AT1 (angiotensin II receptor type 1) and AT2 as well as on its enzymatic conversion by ACE2. Further experiments are needed to establish the pathophysiological consequences of anti-AngII autoantibodies in patients with COVID-19.

Because anti-AngII antibodies developed in response to SARS-CoV-2 infection in hospitalized patients or vaccination with some



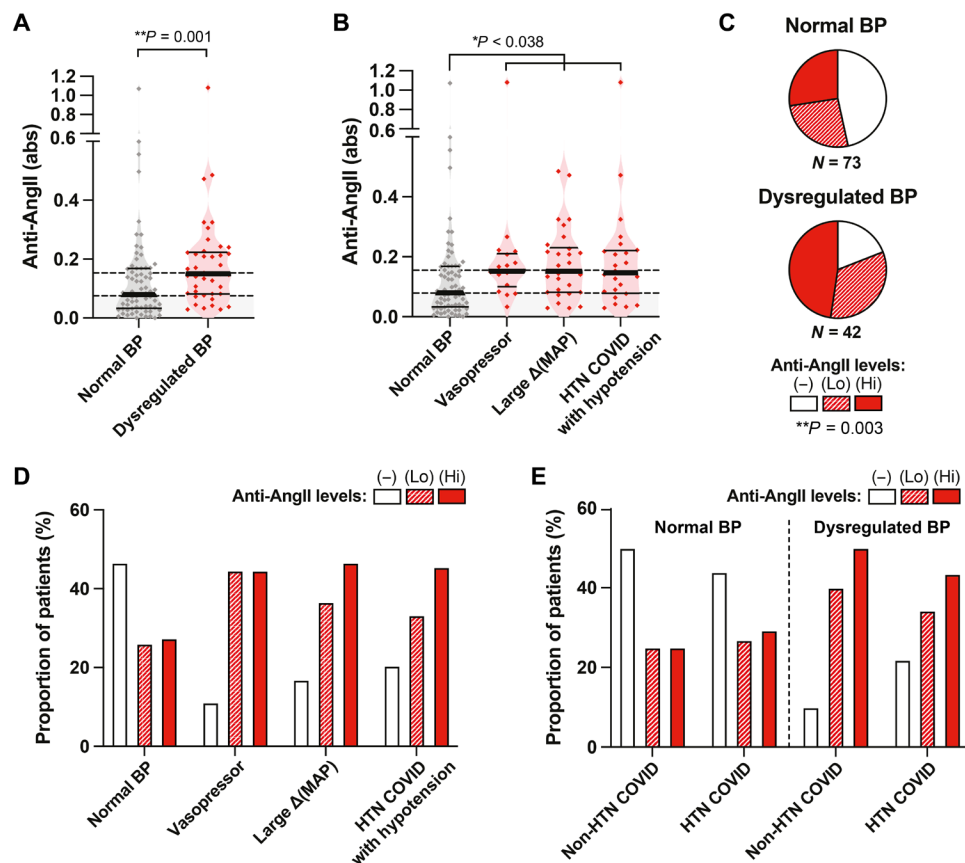


**Fig. 4. Anti-AngII autoantibodies correlates with dysregulated BP and reduced pulse oxymetric saturation  $SpO_2/FiO_2$  (SF ratio) in hospitalized patients with COVID  $N = 115$ .** (Gray threshold indicates positivity of anti-AngII. (A) Anti-AngII levels in the plasma of COVID patients with normal or dysregulated BP (Mann-Whitney test). (B) Levels of anti-AngII antibodies in COVID patients with normal BP as compared to patients with dysregulated BP, categorized as being under vasopressive drugs, exhibiting a large mean arterial pressure variability (large  $\Delta MAP$ ), or having experienced severe acute hypotensive episodes despite their known preexisting HTN condition (these categories are nonexclusive; Kruskal-Wallis test with Dunn's posttest comparison to normal BP). (C) Proportion of patients with normal or dysregulated BP who have negative (-), low (Lo), or high (Hi) levels of anti-AngII antibodies ( $\chi^2$  test). (D) Proportions of patients with negative, low, or high levels of anti-AngII in the COVID patient categories described in (B). (E) Proportions of patients with negative, low, or high levels of anti-AngII in COVID patients with preexisting HTN and/or dysregulated BP.

adjuvants in mice, we hypothesized that anti-AngII antibodies may result from molecular structural mimicry between the AngII peptide and certain epitopes present in Spike or RBD. In that case, anti-AngII and anti-RBD could potentially cross-bind to both antigens. To test this hypothesis, we assessed the binding of two murine IgG monoclonal anti-AngII antibodies (clone E7 and clone B938M) to recombinant SARS-CoV-2 Spike or RBD. We found that both monoclonal anti-AngII antibodies bound to Spike and RBD [but not to an irrelevant protein as the bovine serum albumin (BSA)], although with a lower binding to RBD than to Spike (Fig. 6A). We further demonstrated that the monoclonal anti-AngII antibodies may interfere with AngII binding to its cognate receptor AT1, suggesting that AngII-AT1 signaling could be modulated by the presence of anti-AngII (Fig. 6B).

Conversely, we evaluated the ability of monoclonal anti-RBD antibodies, in a library of those isolated from SARS-CoV-2-infected patients, to bind to AngII. Among the 36 different monoclonal anti-RBD antibodies assessed, 9 showed some low to very low binding to AngII, with one being superior to the others, namely, clone S24-902 (Fig. 6C). We further confirmed the significant although low binding of three of these anti-RBD to AngII, respectively, S24-902, S564-265, and S24-1002, by characterizing their binding at various concentrations (Fig. 6D

and fig. S3A). In contrast, clone S564-14 did not show any specific binding to AngII and was used as a negative control. As expected, the affinities of the monoclonal anti-RBD toward RBD were much higher than toward AngII (fig. S3B). It is not unexpected that the cross-reactivity of anti-RBD to AngII is low, considering that monoclonal anti-AngII also binds weakly to RBD (Fig. 6A) and that AngII is a short eight-amino acid peptide.

We then sought to identify the epitopes of Spike or RBD that lead to cross-reactivity to AngII. To do so, we tested the binding of the two monoclonal anti-AngII antibodies (clones E7 and B938M) to linear epitopes of Spike, using a peptide array that consists of a library of 15-nucleotide oligomer peptides, shifted by five amino acids, covering the full length of Spike. As a control for nonspecific binding, we used the secondary antibody only, in the absence of anti-AngII antibody. Both anti-AngII E7 and B938M clones bound to several linear epitopes on Spike, with a main target at Spike residues aa1146-aa1160 located near the C terminus, outside of RBD (Fig. 6E and fig. S4, A to D; spot J14 on the peptide array), and about 15 secondary targets of lower binding. Five of the secondary peptides targeted by the clone E7 belong to the RBD of Spike, including three more particularly to the receptor-binding motif (RBM) of the RBD (Fig. 6E

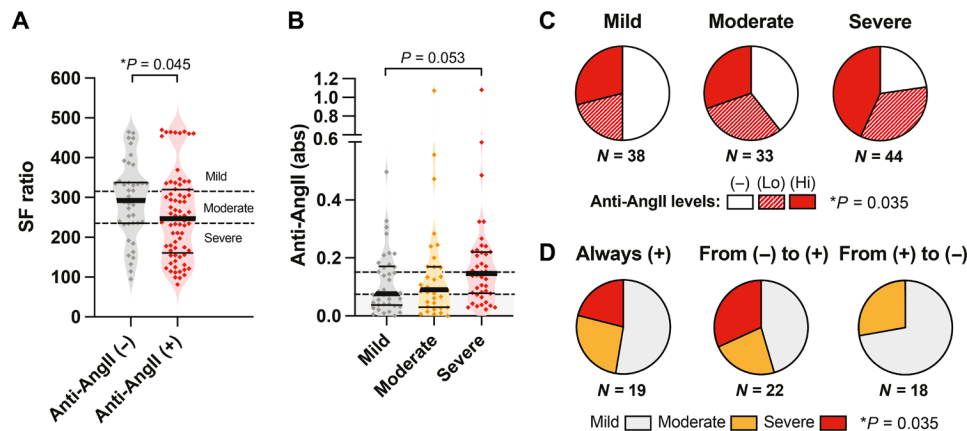


**Fig. 5. Anti-AngII autoantibodies correlates with reduced pulse oxymetric saturation  $\text{SpO}_2/\text{FiO}_2$  (SF ratio) in hospitalized patients with COVID  $N = 115$ .** (A) SF ratio of patients with COVID who are negative (-) or positive (+) for anti-AngII autoantibodies (Mann-Whitney test). SF ratio values are used to define disease severity as being mild, moderate, or severe. (B) Levels of anti-AngII antibodies in patients suffering from mild, moderate, or severe form of COVID, as defined based on SF ratio values (Kruskal-Wallis test with Dunn's posttest). (C) Proportion of patients with negative (-), low (Lo), or high (Hi) levels of anti-AngII antibodies according to their disease severity ( $\chi^2$  test). (D) Of the 75 patients with COVID who were analyzed multiple times after symptoms, proportion of patients who had severe, moderate, or mild disease among patients who were always anti-AngII(+) during their hospitalization [always (+), left], patients who were anti-AngII (-) who turned (+) during their hospitalization [from (-) to (+), middle], and patients who were anti-AngII (+) and who became (-) during their hospitalization [from (+) to (-), right].

and fig. S4A). In contrast, only one peptide targeted by the B938M clone belongs to the RBD region, in the RBM (Fig. 6E and fig. S4B). Notably, although both Spike and AngII share the same receptor—ACE2—their binding to ACE2 occurs at two distinct locations (fig. S5) (12, 13). Most regions targeted by clones E7 and/or B938M have been characterized as being the main B cells epitopes in patients with COVID (colored regions in Fig. 6, E and F, and fig. S4D) (14, 15). These regions, which are likely to contain the epitopes generating anti-AngII autoantibodies, are (i) aa21–aa40, (ii) aa447–aa468, (iii) aa551–aa585, (iv) aa786–aa804, and (v) aa1131–1160 of Spike.

We next compared the Spike epitopes targeted by polyclonal responses raised against RBD/Spike in vaccinated mice or in patients with COVID to the ones targeted by the monoclonal anti-AngII. Thus, we repeated the peptide array assays using anti-AngII(+) or anti-AngII(-) pooled sera from five different mice vaccinated with Spike + MPLA/alum or RBD + MPLA/alum or from five different patients with COVID-19.

We observed that mice raised anti-Spike/RBD antibodies in all regions previously targeted by the monoclonal anti-AngII upon vaccination with Spike+ MPLA/alum (fig. S6A), while mostly in the region aa447–aa468 upon vaccination by RBD + MPLA/alum (fig. S6B). The profiles of anti-AngII(+) and anti-AngII(-) mice were very similar, except for a small increase in binding of anti-Spike to the region aa447–aa468 and anti-RBD to aa551–585, in anti-AngII(+) mice. As to the patients with COVID-19, they raised anti-Spike antibodies against three of the five anti-AngII-targeted regions, namely, aa551–aa585, aa786–aa804, and aa1131–1160, with a slightly higher binding observed to aa786–aa804 in anti-AngII(+) plasma (fig. S6C). Unexpectedly, the region aa1131–1160 was better targeted in anti-AngII(-) plasma; this highlights that not every antibody that binds to anti-AngII-targeting regions would necessarily cross-react with AngII. Together, using monoclonal anti-AngII and anti-RBD antibodies, we demonstrate that antibody cross-binding between AngII and Spike/RBD can occur, even if weakly, which may suggest some structural homology between AngII and certain epitopes of Spike/RBD.

SARS-CoV-2 infection has been shown to induce broad immune dysregulation (16, 17), including generation of wide-ranging autoantibody responses (18). For example, generation of autoantibodies against phospholipids has been shown to contribute to coagulation disorders (19, 20) and against type I interferons to reduced immune response to infection (21). Here, we show that autoantibodies can be generated against AngII, a key regulator of vascular tension. We further show that generation of anti-AngII autoantibodies correlated with disease severity as reflected in dysregulation of vascular tension and lower blood oxygenation. This, along with our *in vitro* signaling data, suggests that the anti-AngII autoantibodies, even if low binding, may be able to interfere with signaling between AngII and its receptors AT1 and ACE2. Some patients with COVID-19 had also been shown to develop autoantibodies against AT1 and ACE2, which similarly correlated with enhanced proinflammatory responses and increased disease severity (22, 23). Such autoantibodies against AT1 and ACE2 have been also observed in patients suffering from other vascular pathologies, particularly in malignant HTN (8) or constrictive vasculopathy (9). Therefore, systematic quantification of autoantibodies against key molecules of the renin-angiotensin pathway (i.e., AngII, AT1, and ACE2), in diseases characterized by vascular dysregulation, including COVID-19, might reveal a common underlying autoimmune etiology. Last, we highlighted the immune epitopes of Spike that could share structural homology with AngII, providing molecular insights in the immune mechanisms that could lead to the generation of anti-AngII autoantibodies upon infection by SARS-CoV-2.

## MATERIALS AND METHODS

### Human plasma biobank and clinical data collection

All sample collection and data recording on patients with COVID-19 were approved by the Institutional Review Board, under an informed consent, from a cohort at the University of Chicago. Serum samples were also collected from both nonhypertensive and hypertensive organ donors provided by the Gift of Hope Organ Donor Network

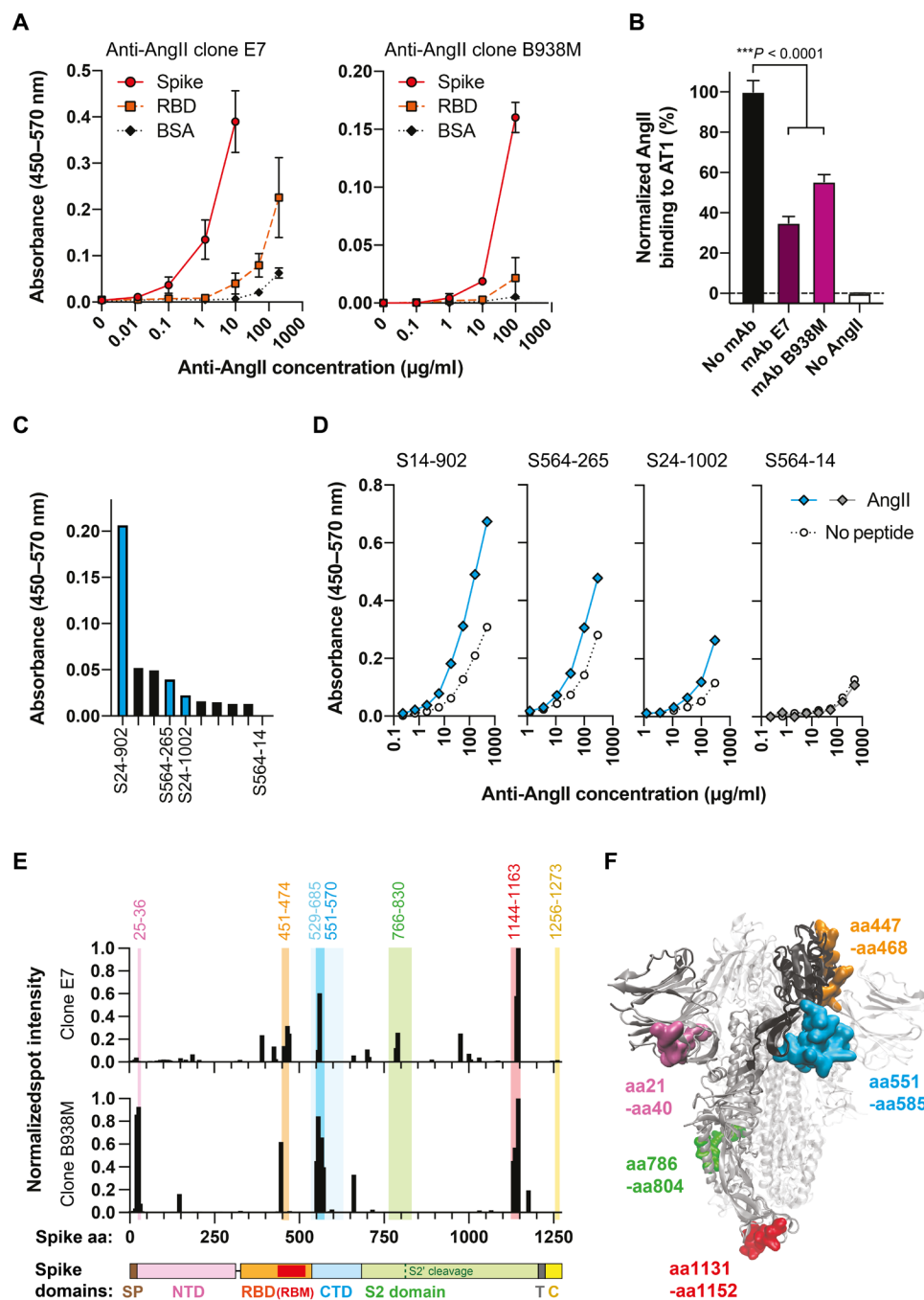


**Fig. 6. Cross-binding of anti-AngII antibodies to the SARS-CoV-2 Spike and RBD antigens.** (A) Binding of two commercial monoclonal anti-AngII (clone E7 and clone B938M) to recombinant Spike and RBD at various concentrations by ELISA. BSA was used as a control for nonspecific binding. (B) Inhibition of AngII binding to its cognate receptor AT1 in the presence of the anti-AngII (clone E7 and B938M) on CHO-AT1 cells, measured by flow cytometry (analysis of variance test with Tukey's posttest). mAb, monoclonal antibody. (C) Binding of a library of monoclonal anti-RBD antibodies against AngII by ELISA (9 of 36 tested showed signals of low binding). (D) Binding of three selected monoclonal anti-RBD (S24-902, S564-265, and S24-1002) to AngII at various concentrations as compared to a non-AngII-binding anti-RBD (S564-14). (E) Binding of monoclonal anti-AngII (clone E7 or B938M) to Spike linear epitopes using a peptide array. Highlighted colored regions represent the most immunogenic and recurrent B cell epitopes of Spike found in patients with COVID [Shrock *et al.* (14) and Li *et al.* (15)], and the associated numbers indicate the amino acid positions that delineate these regions. The x axis represents the full length of Spike (SP, signal peptide; NTD, N-terminal domain; RBD, receptor-binding domain; RBM, receptor-binding motif; CTD, C-terminal domain; NTD, RBD, and CTD together constitute the S1 domain of Spike; T, transmembrane domain; C, cytoplasmic tail). (F) Visualization of the main domains targeted by the monoclonal anti-AngII antibodies on the three-dimensional structure of Spike [Protein Data Bank: 6VXX; (24)]. Domains are highlighted in colors on one monomer of the trimeric Spike structure (RBD is in black; aa#, amino acid position of Spike).

(Itasca, IL). Patients of the COVID cohort were hospitalized patients, in contrast to non-SARS-CoV-2-infected healthy and hypertensive individuals, which were nonhospitalized donors. In addition, many of the patients with COVID-19 had preexisting health conditions, including HTN. Blood was analyzed for the presence and amounts of specific anti-RBD IgG and anti-AngII IgG antibodies by ELISA. Patient data are provided in table S1.

### Titration of anti-RBD antibodies

All procedures using human samples were performed under biosafety level 2 conditions. For the titration of anti-RBD antibodies, ELISA plates were coated with purified recombinant RBD (100 nM) in phosphate-buffered saline (PBS) for 12 to 16 hours at 4°C. Plates were then blocked with 2% BSA in PBS for 2 hours at room temperature. Plates were then extensively washed with PBS with 0.05% Tween (PBST). Human plasmas were diluted at 1:100 in PBST + BSA (0.5%) and then serially diluted by 10. Samples were added to the plates and incubated for 2 hours at room temperature. Plates were washed again and incubated with a horseradish peroxidase (HRP)-conjugated anti-human IgG for 1 hour at room temperature in the dark. Plates were washed, revealed using 3,3',5,5'-tetramethylbenzidine for 30 min in the dark, and the reaction was stopped using 1 M H<sub>2</sub>SO<sub>4</sub>. Absorbances at 450 nm were read using an Epoch plate reader (BioTek) and corrected with the absorbance at 570 nm. Titers represent the highest dilution at which antibodies were detected, in log<sub>10</sub> (e.g., an IgG titer of 4 indicates a detectable level of anti-RBD IgG in a plasma sample diluted at 1:10,000). A value of 0 was given to samples that had no detectable IgG at a dilution of 1:100. Anti-RBD titers are reported in log<sub>10</sub>. Patients were considered positive for anti-RBD when their titers were ≥4, because some healthy donors samples taken before the COVID-19 pandemic had titers of 3. Anti-RBD titers were considered low at 4 to 5 and high at 5 to 8.

### Detection of anti-AngII antibodies

For the detection of anti-AngII antibodies, streptavidin-coated plates were purchased from Pierce (Thermo Fisher Scientific), and biotin-LC-AngII was purchased from AnaSpec. Streptavidin-coated plates were rehydrated using PBST, and biotin-LC-AngII (10 µg/ml) was added to the plate for 2 hours at room temperature. Plates were washed with PBST, and plasma samples diluted at 1:100 were added to the plates for 2 hours at room temperature. Plates were washed again and incubated with an HRP-conjugated anti-human IgG for 1 hour at room temperature in the dark. Plates were washed and developed as previously described, except that the signals were stopped after about 10 to 15 min (when the absorbance of the reference well reached ~1 arbitrary unit). Absorbances at 450 nm were corrected with the absorbance at 570 nm. Detection of antibodies in the absence of biotin-LC-AngII was also performed and subtracted to correct for AngII-unspecific antibody binding. Threshold to define positive signals is 3 SDs above the mean of the healthy donors cohort [after removal of the outliers according to the interquartile range (IQR) rule], which corresponds to an absorbance of 0.077. Threshold to define high levels of anti-AngII is twice the threshold for positivity, which is an absorbance of 0.154.

### Data analysis of anti-AngII and anti-RBD in patients with COVID

Many patients had several plasma samples available at different DPSO. Anti-AngII and anti-RBD levels were measured for all available time

points. As a rule, the highest value of anti-AngII for each patient was selected for data analysis, along with its associated anti-RBD titers at the same time point. The analysis of the anti-AngII/anti-RBD levels changes between early and late time points was performed on the 25 patients who were positive for anti-AngII and had samples available for both time ranges in 1 to 10 and 11 to 20 DPSO. Again, the highest anti-AngII values in 1 to 10 and 11 to 20 DPSO were selected when multiple time points were available, and the anti-RBD corresponded to corresponding time points of highest anti-AngII. For the analysis at >45 DPSO, the highest anti-AngII value detected after 45 DPSO was similarly selected when more than one sample was available for a patient.

The categories for the BMI analysis were chosen according to the Center for disease Control and Prevention definitions: underweight = BMI < 18.5; normal = BMI between 18.5 and <25; overweight = BMI between 25 and <30; obese = BMI between 30 and <40; and severely obese = BMI ≥ 40.

### Data analysis of anti-AngII correlations to BP dysregulation, blood oxygenation, and disease severity

Patients who were considered having a dysregulated BP were (i) the ones who received vasopressive drugs at any time during their hospitalization, (ii) the ones who had large daily fluctuation of  $\Delta$ MAP ≥ 70 mmHg, or (iii) the ones who had preexisting HTN and experienced at least two consecutive days of acute hypotension (MAP < 65 mmHg). For the patients in (ii) and (iii), the dysregulation of BP was assessed in the ±3 days around the time point of the highest anti-AngII value of the patient. Similarly, the SF ratio selected for each patient was the lowest SF ratio value detected in the ±3 days around the time point of the patient's highest anti-AngII value. Disease severity was defined according to the SF ratio value selected for each patient such as: mild disease = SF ratio ≥ 315; moderate disease = SF ratio between 235 and <315; and severe disease = SF ratio < 235.

### Protein productions

The ectodomain of Spike (BEI Resources, NR-52310) or the subdomain RBD (BEI Resources, NR-52309) were cloned into pCAGGS vector for mammalian expression in human embryonic kidney (HEK) 293F suspension cells, as His-tagged recombinant proteins. The proteins were expressed for 4 to 7 days in FreeStyle medium at 37°C, 5% CO<sub>2</sub>, under constant agitation. Cell supernatants were then collected and filtered at 0.22 µm. The proteins were purified by immobilized nickel-affinity chromatography (HisTrap HP column, GE Healthcare) using fast protein liquid chromatography (Äkta Pure system, GE Healthcare). Some protein batches were additionally purified by size exclusion chromatography (Superdex 200 pg column, GE Healthcare) and/or added with 10 mM dithiothreitol to reduce protein dimerization. Proteins were then extensively dialyzed against PBS (pH 7.4), sterile-filtered, and stored at -80°C. All proteins were tested for endotoxin level < 2 EU/mg.

### Vaccine formulation

Vaccines were formulated in PBS by mixing 10 µg of SARS-CoV-2 antigens, i.e., RBD or Spike, with various adjuvants. MPLA/alum was prepared by mixing 5 µg of MPLA (InvivoGen) with 50 µg of alum (InvivoGen). AddaS03 was prepared by mixing 25 µl of AddaS03 (InvivoGen) with 25 µl of PBS containing the SARS-CoV-2 antigens. Mouse-specific stimulatory CpG class B (ODN1826, InvivoGen) was



injected at a dose of 20  $\mu\text{g}$ . Nonadjuvanted groups were composed of 10  $\mu\text{g}$  of antigen only. Mice vaccinated with MPLA/alum without antigens were injected with 5  $\mu\text{g}$  of MPLA and 50  $\mu\text{g}$  of alum.

### SARS-CoV-2 vaccination and analysis in mice

All mouse experimentations were approved by the Institutional Animal Care and Use Committee at the University of Chicago. Female 8-week-old C57BL/6 mice received a prime vaccination using the vaccine formulations above-described, as well as a boost vaccination 3 weeks later. Vaccinations were administered by intradermal injections in the animal hocks in the two forelimbs (25  $\mu\text{l}$  per hock). Mice were bled weekly via the submandibular vein after vaccination for plasma collection and analysis. Anti-AngII IgG levels were determined as described above, except using an anti-mouse total IgG as a detection antibody (1:8000; SouthernBiotech). Threshold to define positive signals is 3 SDs above the mean of the group injected with MPLA/alum without SARS-CoV-2 antigen, which is an absorbance of 0.095. Each experimental group was repeated two to three times independently, and the results showed pooled data from the different experiments. Mice positive for anti-AngII were distributed across the various experiments, and no cage effect has been observed.

### Binding of monoclonal anti-AngII antibodies to RBD and Spike

A mouse monoclonal IgG2a anti-AngII/III clone E7 (MA1-82996; recommended concentration for detection of AngII by ELISA: 5 to 20  $\mu\text{g}/\text{ml}$ ) was purchased from Thermo Fisher Scientific, and a mouse monoclonal IgG1 anti-AngI/II/III (GTX44411; recommended concentration for detection of AngII by ELISA: 10 to 100  $\mu\text{g}/\text{ml}$ ) was purchased from GeneTex. ELISA plates were coated with RBD or Spike (100 nM) in PBS for 12 to 16 hours at 4°C. The plate was then blocked using 2% BSA for 2 hours at room temperature. The anti-AngII antibody was diluted in PBST-BSA (0.5%) at the specified concentrations and added to the plate for 2 hours at room temperature. Binding of the anti-AngII to RBD, Spike, or BSA was detected using an anti-mouse IgG (SouthernBiotech) for 1 hour at room temperature in the dark. The plate was then revealed, and the absorbance was determined as described above.

### Inhibition of AngII binding to AT1 by anti-AngII monoclonal antibodies

Binding of AngII to AT1 receptors was assessed using fluorescently labeled FAM-AngII, purchased from AnaSpec, and Chinese hamster ovarian (CHO) cells expressing recombinant human AT1 (CHO-AT1 cells) were purchased from PerkinElmer. FAM-AngII (100 nM) was preincubated with the anti-AngII monoclonal antibodies (0.3 mg/ml; clone E7 or B938M) in PBS for 30 min at 37°C or with no antibody as a negative control. Then, CHO-AT1 cells were stained with these mixtures in the dark for 20 min on ice. Cells were washed three times in PBS + 2% fetal bovine serum; after that, the binding of FAM-AngII to AT1 on the cell surface was detected using a flow cytometer (BD LSRFortessa, BD Biosciences). The mean fluorescence intensity of the FAM-AngII was computed using FlowJo software.

### Binding of monoclonal anti-RBD to AngII

A library of monoclonal anti-RBD was isolated and sequenced from patients with COVID-19, produced as recombinant proteins using HEK-293 cells, and purified using protein G affinity-based purification. The binding of the monoclonal anti-RBD to AngII was

assessed as described above, by coating the streptavidin-coated plate with biotin-LC-AngII (10  $\mu\text{g}/\text{ml}$ ), washing with PBST, incubating with anti-RBD clones at 20  $\mu\text{g}/\text{ml}$  or indicated concentrations, washing again, and detecting with an anti-human IgG. Negative controls were done in the absence of biotin-LC-AngII.

### Peptide array of SARS-CoV-2 Spike

SARS-CoV-2 Full Spike CelluSpots peptide array assays were purchased from Intavis Bioanalytical Instruments. The assay contains 254 peptides of 15-amino acid length covering the full-length Spike sequence with a shift of 5 amino acids between peptides. The assay was performed as instructed by the manufacturer. Briefly, the membrane was blocked with casein blocking buffer (Sigma-Aldrich) for 4 hours at room temperature and then incubated for 12 hours at 4°C with the anti-AngII clone E7 diluted at a concentration of 20  $\mu\text{g}/\text{ml}$  in casein. The membrane was then washed extensively using PBST and further incubated with an HRP-conjugated anti-mouse IgG (1:5000; SouthernBiotech) for 2 hours at room temperature. The membrane was again extensively washed in PBST and revealed using the Clarity ECL Western substrate (Bio-Rad). The membrane was imaged using a gel imager (Bio-Rad) and spot intensity were analyzed using the Protein Array Analyze for ImageJ (2010) made by Carpentier G and available online at: <https://imagej.nih.gov/ij/macros/toolsets/Protein%20Array%20Analyzer.txt>. For peptide arrays using plasma from patients with COVID-19 or vaccinated mice, the same procedure was followed, except that the pooled plasma from five individuals was diluted at 1:200 in casein and incubated for 4 hours at room temperature instead of the incubation with anti-AngII antibodies. For patient samples, an anti-human IgG was used as a secondary antibody to reveal signals.

### Statistics and software

Graphs and statistical analysis were performed using Prism 9 (GraphPad Software LLC). Median  $\pm$  IQR are represented in violin plots, while mean  $\pm$  SD are represented in other types of graphs. Nonparametric tests (Mann-Whitney for two-group comparisons, Wilcoxon for paired data, and Kruskal-Wallis for >two-group comparisons) were used for data with nonnormal distribution. Spearman tests were used for correlations. Analysis of variance was used for multiple-group comparisons on normally distributed data. All tests were double-sided, and the *P* values were corrected for multiple comparisons. Statistics for  $\chi^2$  proportion tests were performed online using [www.socscistatistics.com](http://www.socscistatistics.com) or [www.icalcu.com/stat/chisqtest.html](http://www.icalcu.com/stat/chisqtest.html) calculators.  $\chi^2$  tests were used to compare the percentage of anti-AngII-positive patients between the different categories of interest. In Fig. 3I,  $\chi^2$  tests were used to compare the percentage of patients with severe disease between the different categories of interest. Threshold for statistical significance was *P* < 0.05. Excel (Microsoft) was used to sort and analyze the data. Molecular structure visualization rendering was done using VMD (Visual Molecular Dynamics 1.9.1). Illustrator CS5 (Adobe) was used to make the figures.

### SUPPLEMENTARY MATERIALS

Supplementary material for this article is available at <https://science.org/doi/10.1126/sciadv.abn3777>

[View/request a protocol for this paper from Bio-protocol.](#)

### REFERENCES AND NOTES

1. K. Kuba, Y. Imai, T. Ohto-Nakanishi, J. M. Penninger, Trilogy of ACE2: A peptidase in the renin-angiotensin system, a SARS receptor, and a partner for amino acid transporters. *Pharmacol. Ther.* **128**, 119–128 (2010).

2. M. Bader, ACE2, angiotensin-(1–7), and Mas: The other side of the coin. *Pflugers Arch.* **465**, 79–85 (2013).
3. F. Alhenc-Gelas, T. B. Drueke, Blockade of SARS-CoV-2 infection by recombinant soluble ACE2. *Kidney Int.* **97**, 1091–1093 (2020).
4. L. Samavat, B. D. Uhal, ACE2, Much more than just a receptor for SARS-CoV-2. *Front. Cell. Infect. Microbiol.* **10**, 317 (2020).
5. P. Verdecchia, C. Cavallini, A. Spannevello, F. Angeli, The pivotal link between ACE2 deficiency and SARS-CoV-2 infection. *Eur. J. Intern. Med.* **76**, 14–20 (2020).
6. B. T. Rouse, S. Sehrawat, Immunity and immunopathology to viruses: What decides the outcome? *Nat. Rev. Immunol.* **10**, 514–526 (2010).
7. J. Mercer, U. F. Greber, Virus interactions with endocytic pathways in macrophages and dendritic cells. *Trends Microbiol.* **21**, 380–388 (2013).
8. M. L. X. Fu, H. Herlitz, W. Schulze, G. Wallukat, P. Micke, P. Eftekhari, K. G. Sjögren, Å. Hjalmarson, W. Müller-Esterl, J. Hoebeke, Autoantibodies against the angiotensin receptor (AT1) in patients with hypertension. *J. Hypertens.* **18**, 945–953 (2000).
9. Y. Takahashi, S. Haga, Y. Ishizaka, A. Mimori, Autoantibodies to angiotensin-converting enzyme 2 in patients with connective tissue diseases. *Arthritis Res. Ther.* **12**, R85 (2010).
10. Q. Li, X. Guan, P. Wu, X. Wang, L. Zhou, Y. Tong, R. Ren, K. S. M. Leung, E. H. Y. Lau, J. Y. Wong, X. Xing, N. Xiang, Y. Wu, C. Li, Q. Chen, D. Li, T. Liu, J. Zhao, M. Liu, W. Tu, C. Chen, L. Jin, R. Yang, Q. Wang, S. Zhou, R. Wang, H. Liu, Y. Luo, Y. Liu, G. Shao, H. Li, Z. Tao, Y. Yang, Z. Deng, B. Liu, Z. Ma, Y. Zhang, G. Shi, T. T. Y. Lam, J. T. Wu, G. F. Gao, B. J. Cowling, B. Yang, G. M. Leung, Z. Feng, Early transmission dynamics in Wuhan, China, of novel coronavirus-infected pneumonia. *N. Engl. J. Med.* **382**, 1199–1207b (2020).
11. X. He, E. H. Y. Lau, P. Wu, X. Deng, J. Wang, X. Hao, Y. C. Lau, J. Y. Wong, Y. Guan, X. Tan, X. Mo, Y. Chen, B. Liao, W. Chen, F. Hu, Q. Zhang, M. Zhong, Y. Wu, L. Zhao, F. Zhang, B. J. Cowling, F. Li, G. M. Leung, Temporal dynamics in viral shedding and transmissibility of COVID-19. *Nat. Med.* **26**, 672–675 (2020).
12. R. Yan, Y. Zhang, Y. Li, L. Xia, Y. Guo, Q. Zhou, Structural basis for the recognition of SARS-CoV-2 by full-length human ACE2. *Science* **367**, 1444–1448 (2020).
13. J. L. Guy, R. M. Jackson, H. A. Jensen, N. M. Hooper, A. J. Turner, Identification of critical active-site residues in angiotensin-converting enzyme-2 (ACE2) by site-directed mutagenesis. *FEBS J.* **272**, 3512–3520 (2005).
14. E. Shrock, E. Fujimura, T. Kula, R. T. Timms, I.-H. Lee, Y. Leng, M. L. Robinson, B. M. Sie, M. Z. Li, Y. Chen, J. Logue, A. Zuiani, D. M. Culloch, F. J. N. Lelis, S. Henson, D. R. Monaco, M. Travers, S. Habibi, W. A. Clarke, P. Caturegli, O. Laeyendecker, A. Piechocka-Trocha, J. Z. Li, A. Khatri, H. Y. Chu; MGH COVID-19 Collection & Processing Team, A.-C. Villani, K. Kays, M. B. Goldberg, N. Hacohen, M. R. Filbin, X. G. Yu, B. D. Walker, D. R. Wesemann, H. B. Larman, J. A. Lederer, S. J. Elledge, Viral epitope profiling of COVID-19 patients reveals cross-reactivity and correlates of severity. *Science* **370**, eabd4250 (2020).
15. Y. Li, M. L. Ma, Q. Lei, F. Wang, W. Hong, D. Y. Lai, H. Hou, Z. W. Xu, B. Zhang, H. Chen, C. Yu, J. B. Xue, Y. X. Zheng, X. N. Wang, H. W. Jiang, H. N. Zhang, H. Qi, S. J. Guo, Y. Zhang, X. Lin, Z. Yao, J. Wu, H. Sheng, Y. Zhang, H. Wei, Z. Sun, X. Fan, S. C. Tao, Linear epitope landscape of the SARS-CoV-2 Spike protein constructed from 1,051 COVID-19 patients. *Cell Rep.* **34**, 108915 (2021).
16. E. J. Giamarellos-Bourboulis, M. G. Netea, N. Rovina, K. Akinosoglou, A. Antoniadou, N. Antonakos, G. Damoraki, T. Gkavogianni, M.-E. Adami, P. Katsaounou, M. Ntaganou, M. Kyriakopoulou, G. Dimopoulos, I. Koutsodimitropoulos, D. Velissaris, P. Koufargyris, A. Karageorgos, K. Katrini, V. Lekakis, M. Lupse, A. Kotsaki, G. Renieris, D. Theodoulou, V. Panou, E. Koukaki, N. Koulouris, C. Gogos, A. Koutsoukou, Complex immune dysregulation in COVID-19 patients with severe respiratory failure. *Cell Host Microbe* **27**, 992–1000.e3 (2020).
17. S. Bhattacharjee, M. Banerjee, Immune thrombocytopenia secondary to COVID-19: A systematic review. *SN Compr Clin Med.* **2**, 2048–2058 (2020).
18. M. Zuniga, C. Gomes, S. E. Carsons, M. T. Bender, P. Cotzia, Q. R. Miao, D. C. Lee, A. Rodriguez, Autoimmunity to Annexin A2 predicts mortality among hospitalised COVID-19 patients. *Eur. Respir. J.* **58**, 2100918 (2021).
19. Y. Zuo, S. K. Estes, R. A. Ali, A. A. Gandhi, S. Yalavarthi, H. Shi, G. Sule, K. Gockman, J. A. Madison, M. Zuo, V. Yadav, J. Wang, W. Woodard, S. P. Lezak, N. L. Lugogo, S. A. Smith, J. H. Morrissey, Y. Kanthi, J. S. Knight, Prothrombotic autoantibodies in serum from patients hospitalized with COVID-19. *Sci. Transl. Med.* **12**, eabd3876 (2020).
20. J. M. Connors, J. H. Levy, COVID-19 and its implications for thrombosis and anticoagulation. *Blood* **135**, 2033–2040 (2020).
21. P. Bastard, L. B. Rosen, Q. Zhang, E. Michailidis, H.-H. Hoffmann, Y. Zhang, K. Dorgham, Q. Philippot, J. Rosain, V. Béziat, J. Manry, E. Shaw, L. Haljasmägi, P. Peterson, L. Lorenzo, L. Bizien, S. Trouillet-Assant, K. Dobbs, A. A. de Jesus, A. Belot, A. Kallaste, E. Catherinot, Y. Tandjaoui-Lambiotte, J. L. Pen, G. Kerner, B. Bigio, Y. Seeleuthner, R. Yang, A. Bolze, A. N. Spaan, O. M. Delmonte, M. S. Abers, A. Aiuti, G. Casari, V. Lampasona, L. Piemonti, F. Ciceri, K. Bilguvar, R. P. Lifton, M. Vasse, D. M. Smadja, M. Migaud, J. Hadjadj, B. Terrier, D. Duffy, L. Quintana-Murci, D. van de Beek, L. Roussel, D. C. Vinh, S. G. Tangye, F. Haerynck, D. Dalmau, J. Martinez-Picado, P. Brodin, M. C. Nussenzweig, S. Boisson-Dupuis, C. Rodriguez-Gallego, G. Vogt, T. H. Mogensen, A. J. Oler, J. Gu, P. D. Burbelo, J. I. Cohen, A. Biondi, L. R. Bettini, M. D'Angio, P. Bonfanti, P. Rossignol, J. Mayaux, F. Rieux-Laucat, E. S. Husebye, F. Fusco, M. V. Ursini, L. Imberti, A. Sottini, S. Paghera, E. Quiros-Roldan, C. Rossi, R. Castagnoli, D. Montagna, A. Licari, G. L. Marseglia, X. Duval, J. Ghosn; HGID Lab; NIAID-USUHS Immune Response to COVID Group; COVID Clinicians; COVID-STORM Clinicians; Imagine COVID Group; French COVID Cohort Study Group; Milieu Intérieur Consortium; CoV-Contact Cohort; Amsterdam UMC Covid-19 Biobank; COVID Human Genetic Effort; J. S. Tsang, R. Goldbach-Mansky, K. Kisand, M. S. Lionakis, A. Puel, S.-Y. Zhang, S. M. Holland, G. Gorochov, E. Jouanguy, C. M. Rice, A. Cobat, L. D. Notarangelo, L. Abel, H. C. Su, J.-L. Casanova, Autoantibodies against type I IFNs in patients with life-threatening COVID-19. *Science* **370**, eabd4585 (2020).
22. A. I. Rodriguez-Perez, C. M. Labandeira, M. A. Pedrosa, R. Valenzuela, J. A. Suarez-Quintanilla, M. Cortes-Ayaso, P. Mayán-Conesa, J. L. Labandeira-Garcia, Autoantibodies against ACE2 and angiotensin type-1 receptors increase severity of COVID-19. *J. Autoimmun.* **122**, 102683 (2021).
23. L. Casciola-Rosen, D. R. Thiemann, F. Andrade, M. I. T. Zambrano, J. E. Hooper, E. Leonard, J. Spangler, A. L. Cox, C. Machamer, L. Sauer, O. Laeyendecker, B. T. Garibaldi, S. C. Ray, C. Mecoli, L. Christopher-Stine, L. Gutierrez-Alamillo, Q. Yang, D. Hines, W. Clarke, R. E. Rothman, A. Pekosz, K. Fenstermacher, Z. Wang, S. L. Zeger, A. Rosen, IgM autoantibodies recognizing ACE2 are associated with severe COVID-19. *medRxiv* 2020.10.13.20211664, (2020).
24. A. C. Walls, Y.-J. Park, M. A. Tortorici, A. Wall, A. T. McGuire, D. Veasler, Structure, function, and antigenicity of the SARS-CoV-2 spike glycoprotein. *Cell* **181**, 281–292.e6 (2020).

**Acknowledgments:** We would like to thank all members from the laboratories of J.A.H. and M.A.S. who participated on COVID research; Y. Zha, H. Jiao, G. G. Li, and S. Yu for biobank COVID sample processing; K. M. Blaine for collecting samples from hypertensive and control donors; and P. Siddarth (University of California Los Angeles, CA, USA) for advice on data analysis. **Funding:** This study was funded by the University of Chicago, through the Chicago Immunoengineering Innovation Center, the Chicago Biomedical Consortium, and the University of Chicago's "Big Ideas Generator" for COVID research. S.J.R. was supported by the T32 CA009566. A.I.S. was supported by NIH R01 AI125644. **Authors contributions:** P.S.B., J.A.H., and M.A.S. designed the study, analyzed the data, and wrote the manuscript. P.S.B. performed the experiments. S.J.R., J.Y., A.R.P., J.T., T.F.G., and A.I.S. collected patient samples and clinical data. S.J.R. processed and analyzed clinical data. H.L.D., C.T.S., S.C., and P.C.W. produced, purified, characterized, and provided the monoclonal anti-RBD antibodies. All authors reviewed the manuscript. **Competing interests:** P.S.B., J.A.H., and M.A.S. are named as inventors on U.S. provisional patent 63/123,199, filed 9 December 2020, relating to the measurement of anti-AngII in immune response. The University of Chicago filed a patent application relating to anti-SARS-CoV-2 antibodies generated by P.C.W., H.L.D., and C.T.S. as coinventors. The authors declare that they have no other competing interests. **Data and materials availability:** All data needed to evaluate the conclusions in the paper are present in the paper and/or the Supplementary Materials.

Submitted 22 November 2021

Accepted 24 August 2022

Published 7 October 2022

10.1126/sciadv.abn3777

## Severe COVID-19 induces autoantibodies against angiotensin II that correlate with blood pressure dysregulation and disease severity

Priscilla S. Briquez, Sherin J. Rouhani, Jovian Yu, Athalia R. Pyzer, Jonathan Trujillo, Haley L. Dugan, Christopher T. Stamper, Siriruk Changrob, Anne I. Sperling, Patrick C. Wilson, Thomas F. Gajewski, Jeffrey A. Hubbell, and Melody A. Swartz

*Sci. Adv.*, **8** (40), eabn3777.  
DOI: 10.1126/sciadv.abn3777

### View the article online

<https://www.science.org/doi/10.1126/sciadv.abn3777>

### Permissions

<https://www.science.org/help/reprints-and-permissions>

Use of this article is subject to the [Terms of service](#)

---

*Science Advances* (ISSN ) is published by the American Association for the Advancement of Science. 1200 New York Avenue NW, Washington, DC 20005. The title *Science Advances* is a registered trademark of AAAS.  
Copyright © 2022 The Authors, some rights reserved; exclusive licensee American Association for the Advancement of Science. No claim to original U.S. Government Works. Distributed under a Creative Commons Attribution NonCommercial License 4.0 (CC BY-NC).